Investigaciones Geográficas
Interuniversity Institute of Geography
University of Alicante
ISSN: 0213-4691 | eISSN: 1989-9890
https://www.investigacionesgeograficas.com

Protection of vineyards from Zonda wind: Evaluation of forest windbreaks. Mendoza, Argentina

Protección de viñedos contra el viento Zonda: evaluación de cortavientos forestales. Mendoza, Argentina

AUTHORSHIP

Rodolfo Dematte
Unidad investigativa epistemología Lógica y Ciencias Básicas Grupo IEMI. Universidad Tecnológica Nacional (UTN), Facultad Regional Mendoza / Instituto de Energías Naturales Renovables CENIIT SECyT, Universidad Nacional de La Rioja, Argentina.

Ernesto Gandolfo Raso
Universidad Tecnológica Nacional (UTN), Facultad Regional Mendoza / Facultad de Ingeniería, Universidad Nacional de Cuyo, Argentina.

Josefina Huespe
Unidad investigativa epistemología Lógica y Ciencias Básicas Grupo IEMI. Universidad Tecnológica Nacional (UTN), Facultad Regional Mendoza / Laboratorio de Física DETI 1 Facultad de Ingeniería, Universidad Nacional de Cuyo, Argentina.

DOI
https://doi.org/10.14198/INGEO.27853

CITATION
Dematte, R., Gandolfo Raso, E., & Huespe, J. (2025). Protection of vineyards from Zonda wind: Evaluation of forest windbreaks. Mendoza, Argentina. *Investigaciones Geográficas*, (83), 91-107. https://doi.org/10.14198/INGEO.27853

CORRESPONDENCE
Rodolfo Dematte (rdematte@gmail.com)

HISTORY
Received: 27 June 2024
Accepted: 5 November 2024
Published: 23 January 2025

TERMS
© 2025 Rodolfo Dematte, Ernesto Gandolfo Raso, Josefina Huespe
This work is published under a license Creative Commons Attribution-NonCommercial-ShareAlike 4.0 International

Abstract

In order to analyze the behavior of the Zonda wind in Mendoza Province, Argentina, the impact of various configurations and levels of optical porosity in forest windbreaks was evaluated. Different configurations of forest curtains were designed, and computational fluid dynamics (CFD) simulations were conducted using OpenFOAM software to assess the protective effect of the windbreaks. The simulations considered the Zonda wind speed type 2 (25 m/s), together with varying levels of optical porosity and geometries of the forest curtains. The results reveal that forest curtains significantly reduce the impact of strong Zonda winds. The effectiveness of these configurations is directly related to the degree of optical porosity (OP) of the forest curtains. A comparison of these findings with the existing literature highlights the importance of OP and the arrangement of forest curtains in mitigating the effects of the Zonda wind. These results corroborate previous studies that have emphasized the crucial role of windbreak structures in protecting agricultural crops from adverse weather conditions. In conclusion, the implementation of forest curtains with a porosity of between 35% and 50% is recommended to achieve effective protection against the Zonda wind in the vineyards of Mendoza. Future research is suggested to further optimize windbreak configurations and improve crop resistance to extreme weather events.

Keywords: windbreak curtains: *vitis vinifera*; shelter effect; CFD; OpenFOAM; Mendoza; Argentina.

Resumen

Para analizar el comportamiento del viento Zonda en la provincia de Mendoza, Argentina, se evaluó el impacto de diversas configuraciones y niveles de porosidad óptica en cortinas forestales. Se diseñaron diferentes configuraciones de cortinas forestales y se realizaron simulaciones de dinámica de fluidos computacional (CFD) utilizando el software OpenFOAM para evaluar el efecto protector de las cortinas. Las simulaciones consideraron la velocidad de viento Zonda tipo 2 (25 m/s), junto con diferentes niveles de porosidad óptica y geometrías de las cortinas forestales. Los resultados mostraron que las cortinas forestales reducen significativamente el impacto de los fuertes vientos Zonda. La efectividad de estas configuraciones estuvo directamente relacionada con el grado de porosidad óptica (PO) de las cortinas forestales. Al comparar

estos hallazgos con la literatura existente, se destacó la importancia de la PO y la disposición de las cortinas forestales en la mitigación de los efectos del viento Zonda. Estos resultados corroboran estudios previos que han subrayado el papel crucial de las estructuras de cortinas en la protección de cultivos agrícolas contra condiciones climáticas adversas. En conclusión, se recomienda la implementación de cortinas forestales con una porosidad entre el 35% y el 50% para lograr una protección efectiva contra el viento Zonda en los viñedos de Mendoza. Se sugiere realizar futuras investigaciones para optimizar aún más las configuraciones de las cortinas y mejorar la resistencia de los cultivos a eventos climáticos extremos.

Palabras clave: cortinas rompevientos: *vitis vinifera*; efecto refugio; CFD; OpenFOAM; Mendoza; Argentina.

1. Introduction

The Zonda wind is a meteorological phenomenon that primarily affects the Andes region in Argentina, especially the province of Mendoza. This wind originates in the Andes mountains and descends eastward, gaining speed and temperature as it descends the mountain slopes (Norte, 1988; Goldberg, 2010). The Zonda wind can have a significant impact on Mendoza's vineyards. Its intense gusts, with speeds ranging between 65 and 120 km/h (Otero, 2018; Norte, 2015), and high temperature can cause damage to the crop, especially during the flowering and growing season of the vine. Plant dehydration, soil moisture loss, and leaf abrasion are some of the problems that can arise due to this wind (Caretta et al., 2004). Additionally, the Zonda can cause wildfires due to its high temperature and dryness (Norte, 2015). In recent years, there has been an increased frequency of Zonda wind events in the province of Mendoza, but there are still no studies directly linking it to climate change but "in 2023, there has already been more Zonda wind than in the last four years" (Lagaglia, 2023, p.1). The annual distribution of Zonda wind occurrences shows a preference for winter and spring with almost no occurrences during summer (Antico et al., 2015).

To protect vineyards from the Zonda wind, viticulturists often implement various measures such as installing natural or artificial windbreaks, proper irrigation to maintain soil moisture, and using crop management techniques that minimize the effects of the wind (Gardiner et al., 2016; Oberschelp et al., 2020; Ramilo, 2022). However, despite these preventive measures, the Zonda wind remains a challenge for viticulture in the Mendoza region. While some studies analyze this phenomenon, they only address the probabilities of damage by the Zonda wind during the flowering of vines and other crops (Caretta et al., 2004), not the effect of windbreak protection on these crops.

This is where windbreaks, also known as shelterbelts or forest curtains, serve a crucial role in protecting vine crops. In this research, we will analyze the importance of windbreaks and their shelter effect on vineyards. The shelter effect created by windbreaks is fundamental for the health and performance of vineyards. These natural or artificial barriers reduce wind speed and create protected areas behind them where vines can develop more optimally. Although windbreaks are widely used, accepted, and adopted, engineering guidelines are lacking to determine the level of performance (i.e., reduction of incident wind speed) they provide to protected areas (Lyu et al., 2020; Miri et al., 2017). Several studies report that the effectiveness of a windbreak is intrinsically related to the flow characteristics in various regions (Judd et al., 1996; Dong et al., 2006; Lyu et al., 2020). Some authors use the d_{20} as a measure to evaluate the shelter effect of windbreaks. The d_{20} is an indicator that shows a correlation between optical porosity and the protective effect, with a 20% reduction in the original wind speed (Judd et al., 1996; Lyu et al., 2020; Wang & Takle, 1997).

This study addresses the understanding of the shelter effect through Computational Fluid Dynamics (CFD) (Wang et al., 2024), as it is a powerful tool for simulating and visualizing fluid flow, such as air, around complex objects. OpenFOAM is a widely used open-source software for performing CFD simulations and is especially suitable for studies in engineering and environmental sciences. Applying OpenFOAM to simulate the shelter effect on crops can provide a detailed understanding of how terrain features affect air flow around plants, which in turn can inform agricultural practices to optimize crop growth and yield (Gonzales et al., 2018; Gonzales et al., 2019; Liu et al., 2018). Combining fluid flow theory with computational simulation technology provides a powerful tool for understanding and harnessing the shelter effect in vineyards, thus contributing knowledge that can significantly improve wine production.

Based on the aforementioned points and considering the economic significance of the Zonda wind's impact in Mendoza, the objective of this research is to evaluate the behavior of the Zonda wind as it interacts with various forest windbreak curtains that protect vine crops. Additionally, this study aims to determine the protective effect of these forest barriers with different configurations and levels of optical porosity. The findings

are intended to provide valuable insights for developing agricultural and forestry management strategies that enhance the sustainability and profitability of crops in areas susceptible to severe winds.

2. Methodology

2.1. Study area

Argentina stands out as a major producer of grapes and wine globally, with a winemaking tradition that dates back centuries (Lacoste, 2019). The Argentine wine industry has experienced notable growth and development in recent decades, consolidating itself as one of the leading countries in the international wine market. Viticulture in Argentina extends throughout the country, from the subtropical regions of the north, such as Salta and Jujuy, to the colder areas of the south, such as Patagonia. However, the most recognized and iconic region of Argentine viticulture is the province of Mendoza, located in the Cuyo region in the west of the country (Figure 1.). Mendoza is responsible for most of Argentina's grape and wine production (Instituto Nacional de Vitivinicultura [INV], 2023).

Figure 1. Map of Argentina, highlighting the province of Mendoza in red color

Source: Tubs (2011)

The province of Mendoza produces 64.23% of the total national grape production and concentrates 74% of the wine produced in Argentina. With 76.14% of the national surface dedicated to grape cultivation, Mendoza has 145,393 hectares distributed in 14,936 vineyards. The vast majority of its production, 99.1%, is destined for wine production, while only 0.9% corresponds to fresh grapes. In addition, 58.2% of the vineyards in the province are cultivated on trellises, which optimizes the quality and yield of the grapes, reaffirming the importance of Mendoza as the main driver of the Argentine wine industry (INV, 2023).

Economically, viticulture and the wine industry play a significant role in the Argentine economy, generating employment, boosting wine tourism, and contributing to the country's exports. Argentine wines are exported to numerous international markets, including the United States, Canada, the United Kingdom, Brazil, and various European and Asian countries (INV, 2023). Wine production is an integral part of the country's cultural and economic identity (Lacoste, 2019). However, the viability of vineyards faces constant challenges, especially in terms of protection against adverse weather conditions, particularly the Zonda wind phenomenon (Goldberg, 2010).

2.2. Numerical simulation

In this section, we describe in detail the materials used and the methods employed to carry out the study of the impact of windbreak curtains and their protective effect (shelter and d_{20}). CFD is chosen because it is a widely validated technique that allows for the simulation and evaluation of wind effects on crops (Hong et al., 2019; Philips & Soligo, 2019; Rosenfeld et al., 2010).

2.2.1. Software

The OpenFOAM software package (version 8), SIMPLE module (Semi-Implicit Method for Pressure-Linked Equations) by Patankar & Spalding (1972), was used as it has been extensively used in research to solve different types of fluid problems to carry out numerical simulations. As mentioned earlier, OpenFOAM is an open-source tool widely used in the scientific community to solve computational fluid dynamics (CFD) problems.

2.2.2 Turbulence Model

The k-epsilon turbulence model was implemented in the simulations. This model was selected due to its ability to capture turbulence in airflows, which is essential for understanding the effect of windbreaks on the shelter phenomenon.

2.3 Model geometry

2.3.1 Windbreaks

The geometry of the windbreak curtain was designed according to the standard specifications used in practical applications (Oberschelp et al., 2020). The forest curtain has an SJ configuration proposed by Wang & Takle (1997, Figure 2). The variety used is *Populus nigra*, widely used as a forest curtain in Mendoza (Food and Agriculture Organization of the United Nations [FAO], 2011; Peri, 2003; Ramilo, 2022).

Figure 2. Forest curtain configuration model proposed by Wang & Takle (1997)

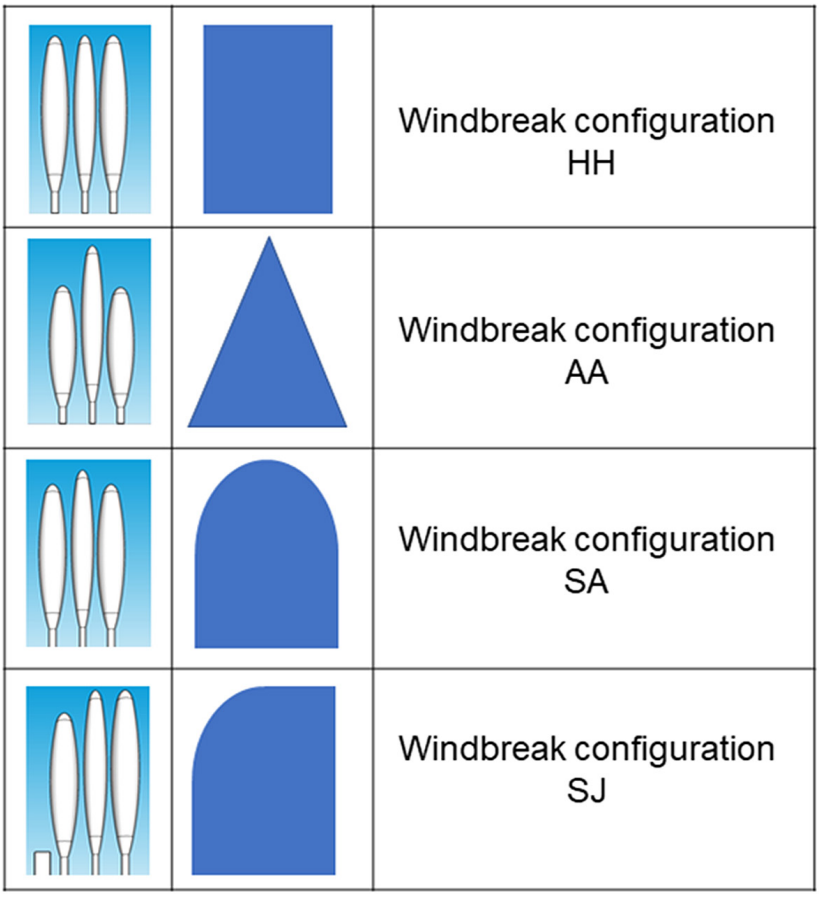

Own elaboration

2.4. Experimental design

Forest barriers can be constructed using various species of shrubs and trees in multiple configurations, thus generating a variety of cross-sectional shapes. In this study, different configurations are used to analyze how the shape of the forest barrier affects the protection effects (Figure 3).

- Test A without windbreak.
- Test B: With a forest barrier with a double row of trees in parallel configuration.
- Test C: With double-row forest barrier interspersed (3 trees first, 4 later).
- Test D: With double-row forest barrier interspersed (4 trees first, 3 later).
- Test E: With triple forest barrier (hedge and three interspersed rows: 4 trees, 3 trees, 4 trees).
- Test F: With triple parallel forest barrier (hedge and three rows of trees in parallel configuration).

Figure 3. Different windbreak configurations

Test		Windbreak configuration
A	without windbreak	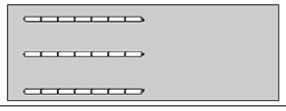
B	double parallel windbreak	
C	double-row windbreak (3 trees, then 4)	
D	double-row windbreak (4 trees, then 3)	
E	triple staggered windbreak with hedge	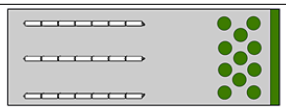
F	triple windbreak parallel with hedge	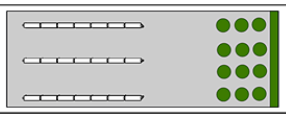

Own elaboration

2.5. Calculation of optical porosity

Optical porosity serves as a natural descriptor of forest curtains (Heisler & DeWalle, 1988). To calculate optical porosity (OP), Equation 1 proposed by Heisler & DeWalle (1988), Miri et al. (2017), Obershelp et al. (2020), Stredová et al. (2012) and Kučera et al. (2020) were used.

$$OP = \frac{(total\ pore\ area)}{(total\ solid\ plant\ area)+(total\ pore\ area)}$$

Equation 1

2.6. Computational domain

The computational domain was defined with dimensions suitable to capture the airflow around the windbreaks. Influential boundary conditions, such as incident wind speed and local atmospheric conditions, were considered. For all simulated cases, the computational domain has dimensions of 40 m in width, 200 m in length, and 40 m in height.

The plant models have 0.85 m high shrub hedges, 6-meter-high plants in the first row and 6.6 meter-high from the second row (H), with an SJ configuration (Wang & Takle, 1997). The separation between each floor is 1.2 m. The cultivation of *vitis vinifera* is organized on low trellises 1.2m high, the planting frame is 1.20 separated between rows of 3m. The distance between the crop and the forest curtain is 2H (13.2 m) (Figure 4).

Figure 4. Model example Test C: double-row forest barrier interspersed (3 trees first, 4 later)

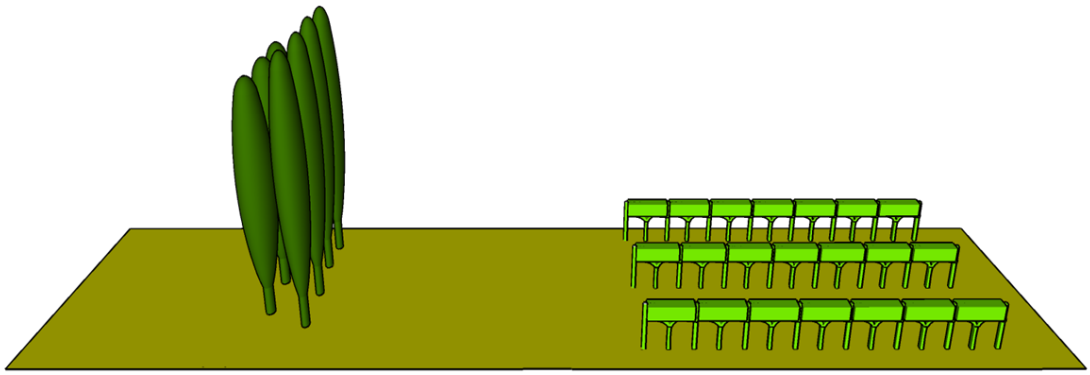

Own elaboration

2.7. Boundary conditions

2.7.1. Flow entry

Inlet conditions were established to simulate the air flow incident on the windbreaks. These conditions were based on real meteorological and statistical data; due to its repeatability, Zonda type 2 wind was chosen for the study, whose maximum speed is 25 m/s (Norte, 2015).

2.7.2. Flow exit

Appropriate exit conditions were applied to guarantee the convergence of the simulations and avoid edge effects in the computational domain.

2.8. Computational meshing

A structured or unstructured computational mesh was generated around the windbreak's geometry and the surrounding domain. Special attention was paid to mesh density and quality to ensure accurate results and proper simulation convergence.

Tests were carried out to verify mesh convergence. The maximum mesh size is 0.125m^3. For the simulation, 2.56 million cells were meshed using the blockMesh® meshes (refinements vary with domain size). In regions close to crops and windbreaks, they were refined using the snappyHexMesh® meshes.

2.9. Simulation procedure

- Preprocessing: a preprocessing stage was carried out to configure the model geometry, define the boundary conditions, and generate the computational mesh.
- Numerical resolution: simulations were performed using appropriate numerical resolution methods, including spatial and temporal discretization schemes.
- Post-processing: a comprehensive analysis of the simulation results was performed with Paraview ®5.6.2 to extract relevant information on the airflow behavior around the windbreaks and the resulting shelter effect. Meanwhile, the wind gradient curves were obtained using GNU Image Manipulation Program (GIMP version 2.10.38)

2.10. Governing equations

High-performance computing resources (Intel core i5 -10400, 2.9 GHz) were used to carry out the numerical simulations due to the complexity of the problem and the need to solve the Navier-Stokes equations to describe the turbulent airflow. The shelter effect is a fluid dynamic phenomenon of great importance that can have significant implications in the distribution of velocity and pressure in the environment of the obstacle, thus affecting the overall behavior of the flow.

The Navier-Stokes Equation is a fundamental tool in fluid mechanics that describes the motion of a viscous fluid. This equation, derived from the fundamental principles of conservation of mass and momentum, together

with Newton's second law for moving fluids, can help us model and predict the shelter effect in different situations. The Navier-Stokes Equation is composed of two main parts: the convective term, which represents the transport of fluid properties due to fluid motion, and the viscous term, which models the diffusion of fluid properties due to viscosity. When considering flow around an obstacle such as forest curtains, these terms are crucial in understanding the shelter effect.

The interaction between these terms in the Navier-Stokes Equation allows us to study how the shelter effect varies depending on the shape and size of the obstacle, as well as the incident flow conditions. The Navier-Stokes equation, together with the k-epsilon turbulence model, was implemented in this OpenFOAM model to simulate turbulent flows representing the zone wind impacting the windbreaks.

The k-epsilon model is one of the most widely used turbulence models in computational fluid dynamics (CFD) due to its balance between accuracy and computational efficiency. In OpenFOAM, this model is implemented to simulate turbulent flows in a wide range of applications. The governing equations in the OpenFOAM k-epsilon model are based on the Reynolds-averaged Navier-Stokes (RANS) equations, and are described as follows:

The formulation of the Navier Stokes equations for incompressible flow together with the k-epsilon model (Equation 2, 3 and 4) in OpenFOAM is:

$$\frac{\partial(\rho U)}{\partial t} + \nabla.(\rho UU) = -\nabla p + \nabla.(\mu \nabla U) - \rho g - \rho \varepsilon k \qquad \textit{Equation 2}$$

Where:
ρ is the density of the fluid
U is the velocity vector
p is the pressure
g is the gravitational acceleration vector
ε is the turbulence dissipation rate
k is the turbulent kinetic energy

Regarding the turbulence dissipation rate ε and the turbulent kinetic energy k

$$\frac{\partial(\rho k)}{\partial t} + \nabla.(\rho Uk) = \nabla.[(\frac{\mu_t}{\sigma_k} + \frac{\mu}{\sigma_k})\ \nabla k] + P_k - \rho \varepsilon C_{\epsilon_1} k + \nabla.(\rho UU).U - \rho \varepsilon C_{\epsilon_2} \frac{k^2}{\epsilon} \qquad \textit{Equation 3}$$

$$\frac{\partial(\rho \epsilon)}{\partial t} + \nabla.(\rho U\epsilon) = \nabla.[(\frac{\mu_t}{\sigma_\epsilon} + \frac{\mu}{\sigma_\epsilon})\ \nabla \epsilon] + C_{\epsilon_1} \frac{\epsilon}{k} P_k - C_{\epsilon_2} \rho \frac{\epsilon^2}{k} + \rho \varepsilon C_{\epsilon_1} k - \rho \epsilon C_{\epsilon_1} k - \rho C_{\epsilon_1} \frac{\epsilon}{k} \nabla.(\rho UU) \qquad \textit{Equation 4}$$

Where:
μ_t is the turbulent viscosity
σ_k and σ_ϵ are Prandtl coefficients
P_k is the rate of turbulent kinetic energy production
$C_{\epsilon 1}$ and $C_{\epsilon 2}$ are constants of the k-ϵ model

These equations, together with the boundary and initial conditions, are those that are solved numerically in the model used in OpenFOAM to obtain the solution of the turbulent flow.

These equations represent the conservation of turbulent kinetic energy and the dissipation of turbulent energy, respectively. In OpenFOAM, these equations are solved numerically together with the mass and momentum conservation equations to predict the behavior of turbulent flow in a given domain. Additional terms, such as turbulent kinetic energy production and turbulent energy dissipation, are modeled using empirical hypotheses and relationships that depend on the specific flow and geometry.

3. Results

3.1. Windbreak optical porosity

The optical porosity of the forest curtain and the classification it based on permeability are shown in Table 1 (Wang & Takle, 1997). Optical porosity is associated with the different geometric configurations of the forest curtains.

Table 1. Optical porosity of the tests conducted

Test	Optical porosity	Classification
Test A: Without forest barrier.	100.00%	Permeable
Test B: With a forest barrier with a double row of trees in parallel configuration	53.75%	Permeable
Test C: With double-row forest barrier interspersed (3 trees first, 4 later).	36.71%	Semi-permeable
Test D: With double-row forest barrier interspersed (4 trees first, 3 later).	36.71%	Semi-permeable
Test E: With triple forest barrier (hedge and three interspersed rows: 4 trees, 3 trees, 4 trees).	28.26%	Semi-permeable
Test F: With triple parallel forest barrier (hedge and three rows of trees in parallel configuration).	43.20%	Semi-permeable

Own elaboration

3.2. Evaluation of the protection effect of windbreaks

This study analyzes the protective effect of windbreaks through various tests with different windbreak configurations that compare the behavior of category 2 Zonda wind at a speed of 25 m/s. (Figure 5). In the bibliography, H represents the height of the forest windbreak or barrier used in the tests. The relationship between this height and the distance of the protective effect in reducing wind speed is measured in terms of units of H (Judd et al., 1996; Lyu et al., 2020; Wang & Takle, 1997). As the crops are vineyards with low trellises, which are 1.2 meters high, a protection height of 1.5 meters is considered in this research.

Figure 5. Protection distances from the forest curtain. Comparative study between different tests. Graphic made in Origin software®

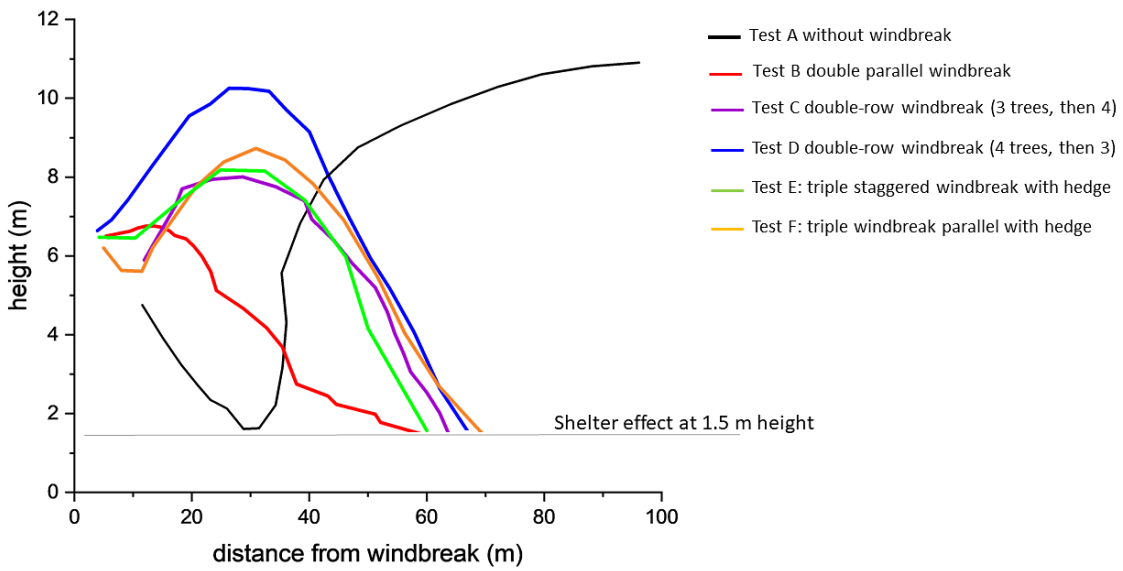

Own elaboration

In Test A, where no forest curtains are present (100% optical porosity), the wind impacts directly, resulting in no significant reduction in speed (Figure 6). The results of all conducted tests are illustrated in the graphs shown in Figures 7, 8, 9, 12, and 13.

Tests C (Figure 7) and D (Figure 8), both double rows of interspersed trees (optical porosity of 36.71%), have similar results, equivalent to between 10H (66 m) and 11H (72 m) respectively. This configuration significantly reduces wind speed and protects crops, reducing the direct impact of Zonda wind category 2. The alternation of 3 and 4 trees provides a structure allowing air circulation, avoiding damage from too strong winds while maintaining an effective barrier.

Meanwhile, Test E (Figure 12), with an optical porosity of 26.71% (triple row interspersed with hedges), yields similar results to Test B (Figure 9), which has a porosity of 53.75% (9H, 60 m).

In the case of the F test (Figure 13), optical porosity of 43.20% (three rows in parallel with hedge) has a protective effect of 76 m 12H (Figure 5).

3.3. Comparisons between tests

The comparisons aimed at evaluating the relative effectiveness of different windbreak configurations (Table 2). These comparisons will provide insight into how different windbreak configurations influence protection against severe wind events like Zonda 2, helping to optimize windbreak design for agricultural and environmental applications.

Table 2. Comparisons made between tests

Test	Detail
Test A (no forest curtain control)	This test served as a basis for understanding natural wind exposure without any windbreak intervention.
Test C vs. D	Comparison between different configurations of double interspersed row of windbreaks to determine which one provides better protection against Zonda 2 wind.
Test C vs. B	Evaluation of the effectiveness of the windbreak comparing different interleaved versus parallel configurations.
Test E vs. F	Comparison focused on the protection of triple row windbreaks with a hedge to establish the protected area.
Test F vs. C	Evaluation of the effectiveness of the parallel triple row windbreak with hedge versus double interspersed row
Test E vs. C	Evaluation of the effectiveness of the triple row windbreak interspersed with hedge versus double row interspersed without hedge

Own elaboration

3.3.1. Test A

Test A is a control test conducted without a forest barrier to observe how the wind behaves without a windbreak. The wind directly impacts the crop at a speed of 25 m/s, equivalent to a Zonda category 2 wind (Norte, 2015). The optical porosity of 100% is equivalent to not having any type of barrier to protect from the wind. This wind would affect the entire plantation during the flowering and fruiting period; it would cause the total harvest loss and physically damage the plant severely; in many cases, the plants are left with bare roots (Figure 6).

Figure 6. Test A. Wind behavior and speed in crop fields without forest curtains. Graphic made in Paraview software®. Prepared based on the results obtained

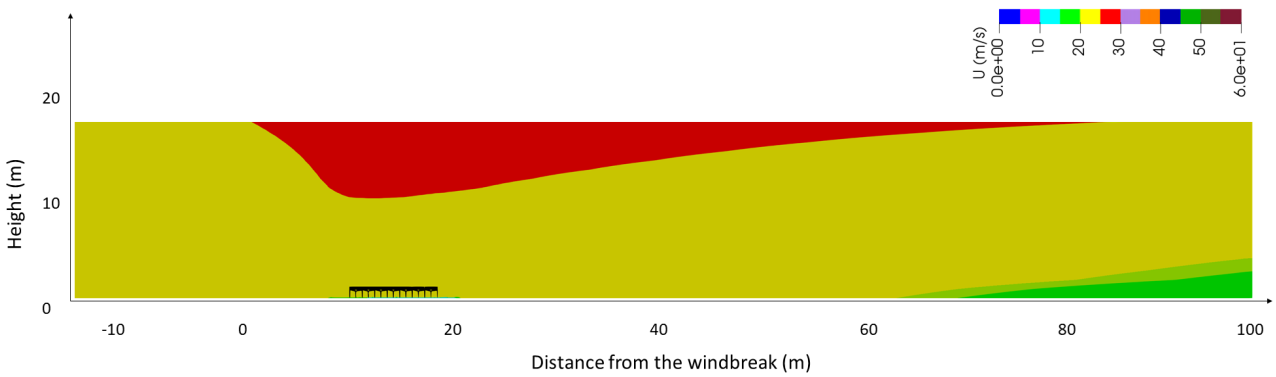

Own elaboration

3.3.2. Test C versus Test D

In the windbreak tests, we compared Test C, which featured a double interspersed row of trees (3 trees initially, followed by 4), with Test D, where the configuration was reversed (4 trees initially, followed by 3). These tests aimed to assess the effectiveness of different tree arrangements in providing windbreak protection.

The porosity of both barriers is 36.71%, which makes it considered a semi-permeable barrier. The results show that an alternating configuration reduces the impact of the Zonda wind by 25 m/s. In addition, it offers a protective effect on the crop at a 1.5 m height that extends a distance of 10 H for test C and 11 H for test D, which is equivalent to 66 and 72 m, respectively (Figure 7 and Figure 8).

Figure 7. Test C. Behavior and wind speed (U=25m/s) in crop fields with two-row forest curtains interspersed without hedges with optical porosity of 36.71%. Graphic made in Paraview software®. Prepared based on the results obtained

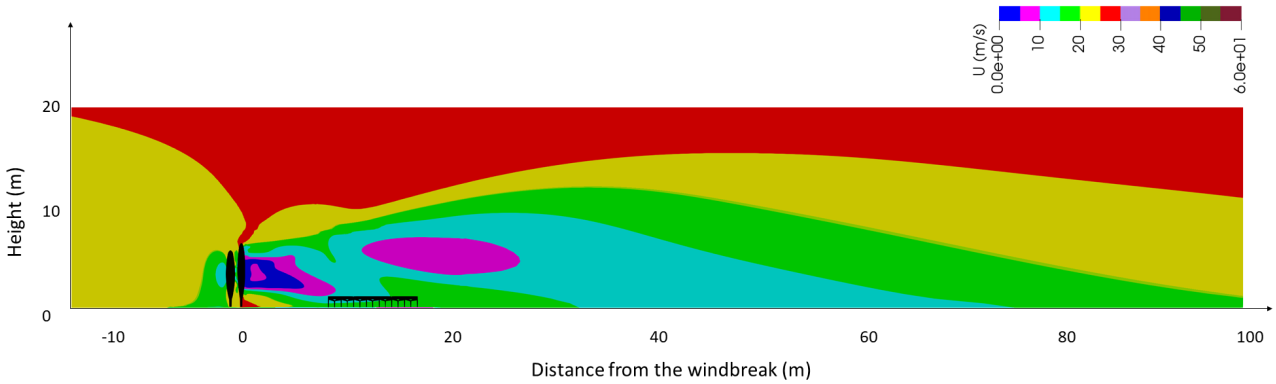

Own elaboration

Figure 8 Test D. Behavior and wind speed (U=25m/s) in crop fields with two-row 4 x 3 forest curtains interspersed without hedges with optical porosity of 36.71%. Graphic made in Paraview software®. Prepared based on the results obtained

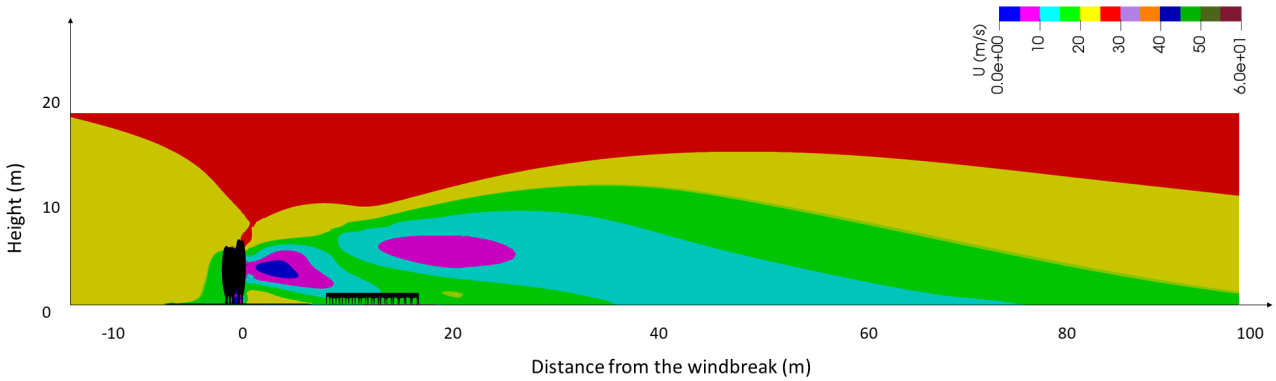

Own elaboration

3.3.3- Test C versus Test B

In Test C (Figure 7) the protective distance is greater, resulting in fewer internal gusts exceeding speeds of 20 m/s. At a height of 1.5 m, the protected area in Test C extends approximately 66 m from the windbreak (10H). In contrast, Test B (Figure 9) shows a shorter protected area at the same height, covering about 56 m lengthwise (9H). Both tests can be verified in the top view graphs that show the shelter effect on the crop surface at a height of 1.5 m (Figure 10 and 11).

Figure 9. Test B. Behavior and wind speed (U=25 m/s) in crop fields with two-row forest curtains without intercropping without hedges with optical porosity of 53.75%. Graphic made in Paraview software®. Prepared based on the results obtained

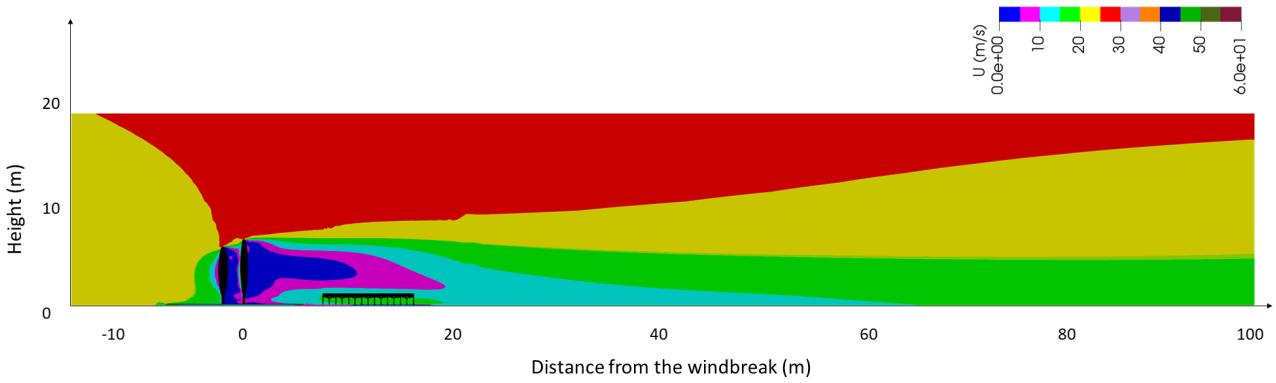

Own elaboration

Figure 10. Test B behavior and wind speed (U=25 m/s) in crop fields with two-row forest curtains without intercropping without hedges with optical porosity of 53.75% View at Z=1.5 m height from level ground. Graphic made in Paraview software®. Prepared based on the results obtained

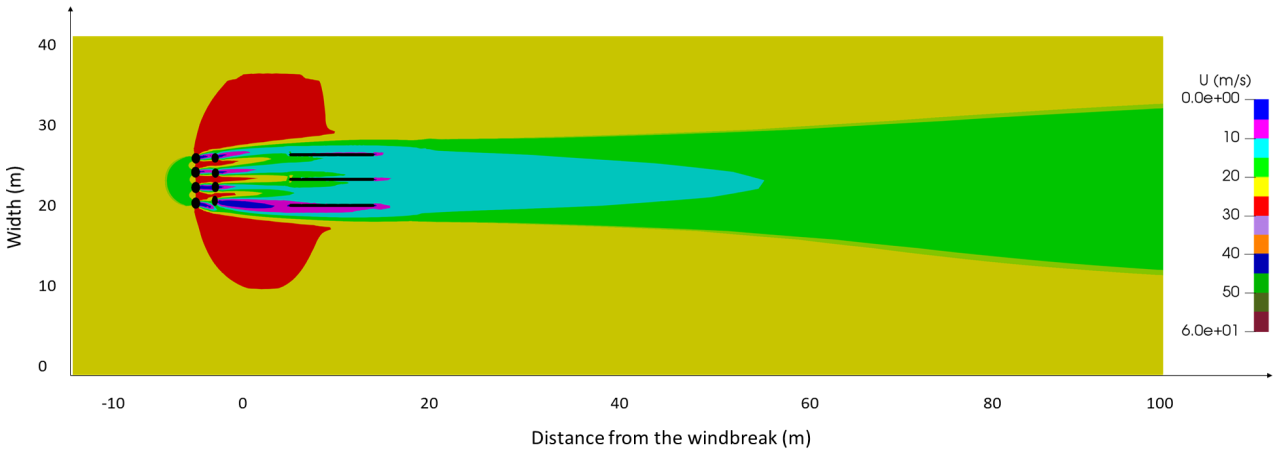

Own elaboration

Figure 11. Test C. Behavior and wind speed (U=25 m/s) in crop fields with two-row forest curtains interspersed without hedges with optical porosity of 36.71% View at Z=1.5 m height from plant level floor. Graphic made in Paraview software®. Prepared based on the results obtained

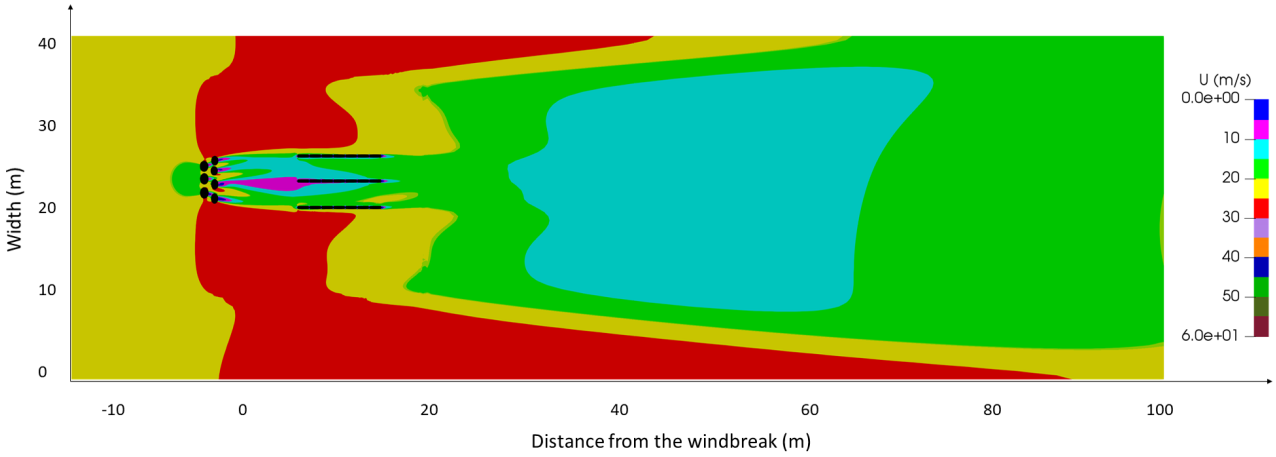

Own elaboration

3.3.4. Test E versus Test F

In the case of test E (optical porosity 28.26%), the protection distance is less than test F (optical porosity 43.20%), but it presents greater stability. Within the protection effect the speeds are less than 15 m/s, providing a greater barrier. dense and stable. The protection distance is equivalent to 9H, useful for the case of plantations with little extension and with severe Zonda events (Figure 12 and Figure 13).

Figure 12. Test E. With triple forest barrier (hedge and three interspersed rows: 4 trees, 3 trees, 4 trees) behavior and speed of the wind (U=25m/s) in crop fields with forest curtains of three rows interspersed with hedges with optical porosity of 28.26%. Graphic made in Paraview software®. Prepared based on the results obtained

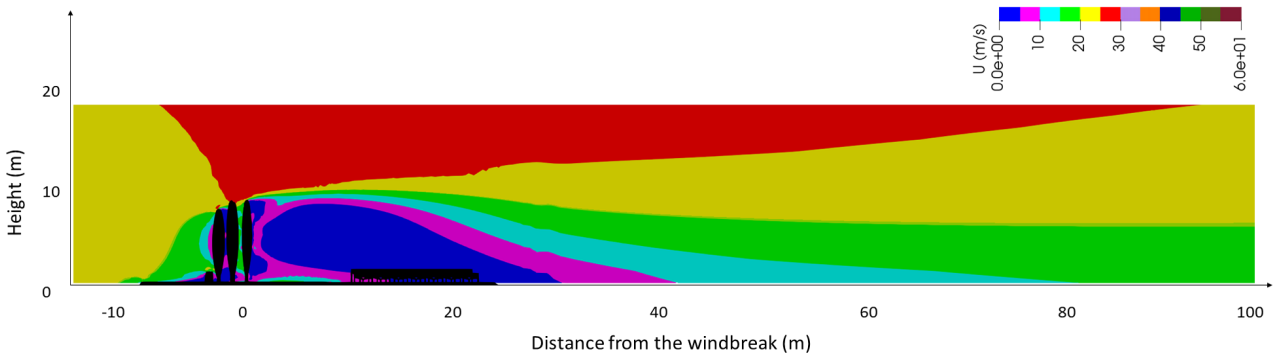

Own elaboration

Figure 13. Test F. Behavior and wind speed (U=25m/s) in crop fields with forest curtains of three parallel rows not interspersed with hedges with optical porosity of 43.20%. Graphic made in Paraview software®. Prepared based on the results obtained

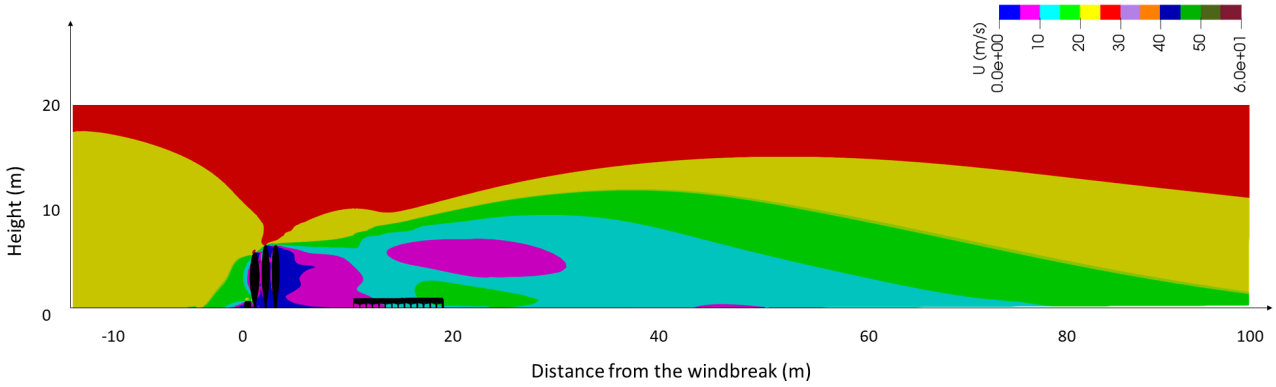

Own elaboration

In the case of test F, the protection distance is greater but there are internal gusts of high speeds greater than 15 m/s, the protection distance extends up to 12H, useful for the case of large plantations but in light zonda events (Figure 14 and 15).

Figure 14. Test E behavior and wind speed (U=25 m/s) in crop fields with forest curtains of three rows interspersed with hedges with optical porosity of 28.26% View at Z=1.5 m height from ground level. Graphic made in Paraview software®. Prepared based on the results obtained

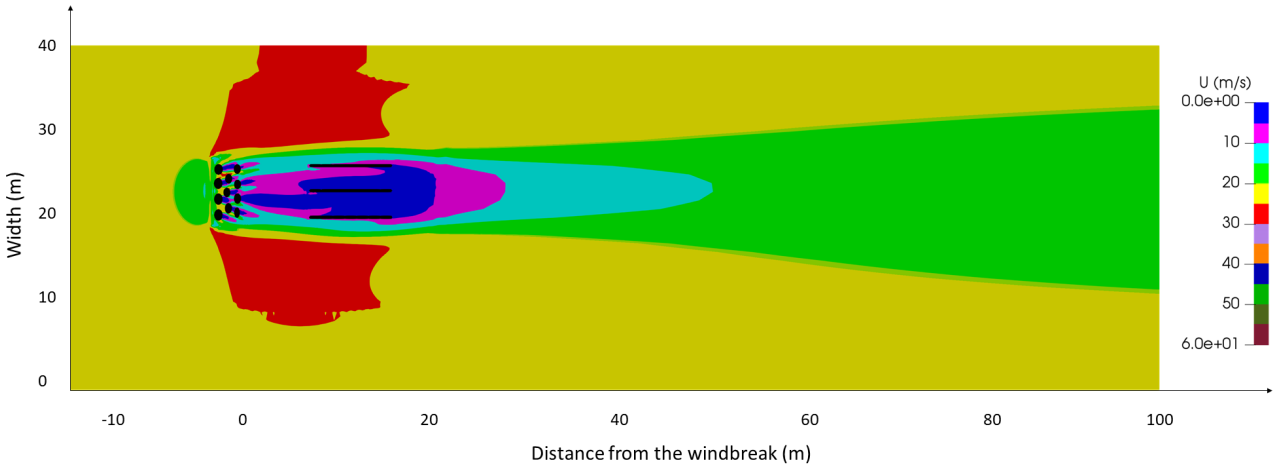

Own elaboration

Figure 15. Test F. Behavior and wind speed (U=25m/s) in crop fields with forest curtains of three parallel rows not interspersed with hedges with optical porosity of 43.20% top view cut at Z= 1.5m. Graphic made in Paraview software®. Prepared based on the results obtained

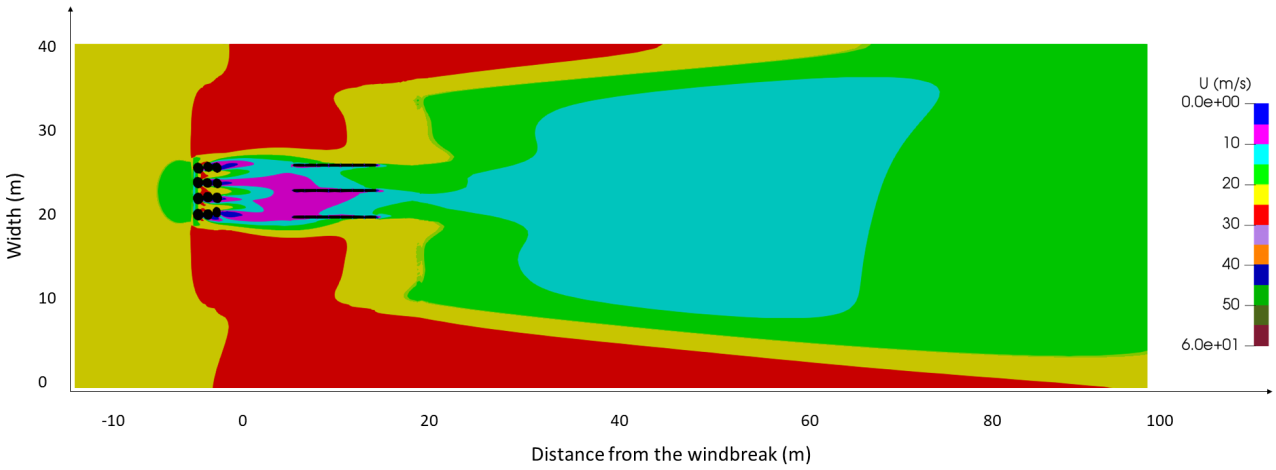

Own elaboration

3.3.5. Test E versus Test C

In this case, both tests are compared with different porosities. In the case of test E (Figure 12 and 14) the protection distance is smaller and there is more stability and protection, for speeds less than 10 m/s the protection distance is equivalent to 9H, this information is useful in the case of small plantations and strong zonda events. In the case of test C (Figure 7 and 11) the protection distance is greater but there are internal gusts of high speeds greater than 15 m/s; The protection distance is equivalent to 10H applicable in the case of large plantations, since due to the configuration vorticities are generated that nullify the protective effect but it is useful for mild zonda events.

3.3.6. Test F versus Test C

In the case of test C (Figure 7 and Figure 11), the protection distance equivalent to 10H applicable in the case of large plantations but mild Zonda events was previously analyzed. In the case of test F (Figure 13 and 15) the protection distance is greater but there are internal gusts with speeds greater than 15 m/s. The protection distance is equivalent to 12H. In both cases, these types of windbreaks are useful in the case of large plantations but only in areas where there is a predominance of slight windbreak events at low speeds (Figure 11 and 15).

3.4. Protection distance d_{20}

In simple terms, d_{20} indicates the distance at which the wind speed reduction reaches 20%. This measure is used to evaluate the effectiveness of windbreaks or forest barriers in mitigating wind speed and protecting areas behind them. Although the d_{20} were calculated, for our case study it has no applications because a 20% reduction in the speed of Zonda analyzed would still have harmful effects on the crops, the optimal speed is less than 15 m/s (Table 3)

Table 3. Protection distance d_{20}

Test	Optical Porosity	Protection distance d_{20}
A	100.00%	No show
B	53.75%	between 60-100 m
C	36.71%	between 70-100 m
D	36.71%	between 80-100 m
E	28.26%	between 55-100 m
F	43.20%	between 78-100 m

Own elaboration

It can be seen by analyzing the d_{20} that there is a correlation between optical porosity and the protective effect in the 20% reduction in wind speed. It is observed that as the optical porosity decreases (that is, the windbreak has a greater frontal surface), the value of d_{20} tends to increase. This means that windbreaks with lower optical porosity have a greater ability to reduce wind speed at greater distances from the windbreak.

4. Discussion

4.1 Protection distance d_{20}

Several authors mention about the protection distance d_{20} for forest curtains (Wang & Takle, 1997; Judd et al., 1996; Hong et al., 2019), in our case study it is not applicable because the high wind speeds Zonda (25m/s), a 20% decrease still affects the plantation, causing structural mechanical damage and loss of productive capacity. Furthermore, it is estimated that the 20% reduction in wind speed, known as d_{20}, is not applicable to the Zonda wind due to its intensity.

4.2. Wind behavior

In all the cases analyzed they show the behavior scheme of the wind against forest curtains, to a lesser or greater extent they approximate the image (Figure 16), the variation is related to the percentage of optical porosity of the windbreak curtain.

Figure 16. Scheme of velocity regions in forest curtains

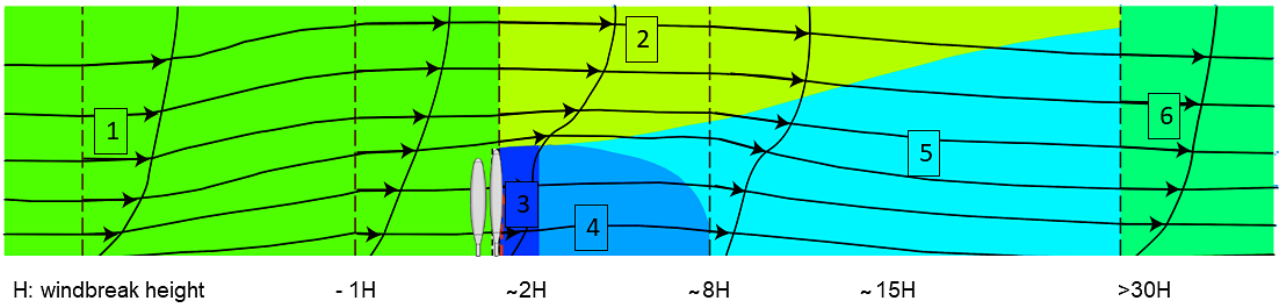

Source: Judd et al. (1996) and Lyu et al. (2020). Own elaboration

Judd et al. (1996) and Lyu et al. (2020) explain that region 1 is the approach flow that impacts the forest curtain, generating two clearly differentiated zones; region 2, a displaced flow resulting from the collision of the wind with the forest curtain; in turn, there is region 3, which is the purge flow, what passed through the porosity of the forest curtain, the zone 4 is backwater zone where the velocities reduce and the shelter effect of the curtain is seen, a zone 5 where there is a transition zone until the initial force of region A which is called rebalancing zone (zone 6).

The protection zones usually extend between 2H and 8H. Where H is the height of the curtain. Many authors maintain that the size of these regions maintains a certain proportionality with H (which is why it is taken as a normalized variable). The distortion of this scheme is associated with porosity; when this increases, zone 4 is reduced (Lyu et al, 2020)

This effect is more notable in curtains with a medium porosity, where a significant decrease in wind speed is observed, crucial to maintain adequate pollination conditions and plant resistance.

Yukhnovskyi et al. (2020) found that the effectiveness of optical porosity in windbreaks ranges between 40% and 50%, a finding supported by the experimental studies of Hong et al. (2015). However, it is important to consider that excessive densities in the vegetation of the curtains can counterproductively reduce the protected area, as indicated by previous studies (Heisler & DeWalle, 1988; Obershelp et al., 2020).

It was found that speeds greater than 15 m/s can cause significant damage to crop, including soil erosion and loss of plant material. For future studies, additional variations in wind speed will be explored to determine the optimal configuration of windbreaks that maximizes their effectiveness in protecting crops.

4.3. Windbreak configuration and shelter effect

The tests are classified based on their effectiveness in reducing wind impact, measured in multiples of H (height of the protection structure). Tests C, D, and F demonstrate significant effectiveness, ranging from 10H to 12H, whereas Test E and Test B show moderate effectiveness at 9H. Test A, without any protective curtains, shows minimal effectiveness, emphasizing the importance of optical porosity in windbreak configurations.

This relates to the effectiveness of windbreaks (as discussed in the mentioned studies) in reducing wind speed and protecting crops. Windbreaks can create significant air flow reduction zones, for example, from 10H to 15H in the lee wake zone (Hong et al., 2019). This reduction in air flow is crucial for protecting crops against direct wind impacts, especially in adverse weather conditions such as Zonda category 2 winds.

The study showed that forest windbreaks are effective in mitigating the effects of the Zonda wind, a severe climatic phenomenon in Mendoza with speeds that can reach up to 25 m/s. The different configurations of curtains, evaluated by their porosity and arrangement with respect to the prevailing wind, show that these structures are capable of significantly reducing the speed and modifying the direction of the wind in the protected area, known as the shelter effect.

The results obtained in this study on the effectiveness of forest windbreaks to mitigate the impact of the Zonda wind on vineyards in Mendoza are applicable to other agricultural regions with similar climatic conditions, such as the provinces of La Rioja, San Juan, Catamarca, Salta, and Jujuy, in areas near the Andes Mountains in Argentina (Norte, 2015). These regions experience not only strong, dry winds with characteristics like the Zonda, but also extreme temperature fluctuations, low humidity, and occasional dust storms, all of which can negatively affect crop yields and quality (Goldberg, 2010).

The implementation of forest windbreaks has been shown to reduce wind speed, protect soil from erosion, and minimize temperature fluctuations at the canopy level, thus helping to maintain optimal conditions for vine growth, aligning with the results presented by Hong et al. (2019), which demonstrate that windbreaks effectively enhance airflow patterns and microclimatic conditions, further benefiting crop productivity.

The findings suggest that these strategies can help reduce water stress and physical damage to crops, particularly during the critical stages of growth and fruiting. Moreover, the use of computational fluid dynamics (CFD) simulations to predict the behavior and protective effects of windbreaks adds a quantitative analysis, reinforcing the applicability of these strategies to a variety of crops beyond vineyards.

These examples demonstrate that such strategies are not only relevant for Mendoza but can also provide significant benefits to farmers in other regions of Argentina near the Andes, as well as to researchers seeking to optimize wind protection measures for agriculture in similar climates worldwide.

5. Conclusions

Based on the results obtained to evaluate the protective effect of various configurations of windbreak curtains, each with different levels of porosity, it is concluded that forestry curtains represent an effective measure of protection against the Zonda wind, known for its extreme speeds, that reaches up to 25 m/s, the most common event in the Mendoza region. The structure of the curtain, oriented perpendicular to the prevailing wind, causes a speed reduction and flow diversion effect, creating a shelter area that protects crops located up to 12H behind the curtain, depending on its configuration. and optimal porosity.

The interaction of the wind with the forest curtain produces a partial filtration through the interstices between the plants, which reduces their speed. Simultaneously, a portion of the wind is deflected around the front surface of the curtain. These changes in wind speed and direction are attributable to the resistance offered by the plants of the forest curtain. The protected area, known as the “refuge effect”, experiences a significant reduction in wind speed, creating an environment where crops are less exposed to wind impact. This protection zone extends between 6H and 12H, depending on the configuration and optical porosity of the curtain. It is notable that windbreaks with medium, optical porosity fulfill a crucial protective effect during intense gusts of wind.

The results clearly demonstrated that the forest curtains are effective in controlling the Zonda wind, reducing its impact in all the configurations analyzed. When the wind hits the forest curtain, part of it filters through the gaps, losing speed, while another part is deflected by the front surface of the curtain. These changes in wind speed and direction are a consequence of the resistance offered by the plants of the forest curtains.

The study also noted that very dense curtains may not be effective, as they can divert wind flow upwards and reduce the protected area behind them. These observations are consistent with previous studies that warn of the counterproductive effects of curtains that are too dense in certain contexts.

References

Antico, P. L., Chou, S. C., & Mourão, C. (2015). Zonda downslope winds in the central Andes of South America in a 20-year climate simulation with the Eta model. *Theoretical and Applied Climatology, 128*(1-2), 291–299. https://doi.org/10.1007/s00704-015-1709-2

Caretta, A., Ortega, A., & Ortíz Maldonado, A. (2004). Probabilidades de daño por viento Zonda en la floración de frutales, vid y olivos. *Revista de la Facultad de Ciencias Agrarias UNCuyo, 36*(2), 49-58. http://bdigital.uncu.edu.ar/82

Dong, Z., Qian, G., Luo, W., & Wang, H. (2006). Threshold velocity for wind erosion: The effects of porous fences. *Environmental Geology, 51*(3), 471–475. https://doi.org/10.1007/s00254-006-0343-9

Food and Agriculture Organization of the United Nations (FAO). (2011). *Evaluación de la desertificación en Argentina: Resultados del Proyecto LADA/FAO*. Secretaría de Ambiente y Desarrollo Sustentable de la Nación. https://www.fao.org/fileadmin/templates/nr/documents/LADA_docs/Libro_LADA_COMPLETO.pdf

Gardiner, B., Berry, P., & Moulia, B. (2016). Review: Wind impacts on plant growth, mechanics and damage. *Plant Science, 245*, 94–118. https://doi.org/10.1016/j.plantsci.2016.01.006

Golberg, A. D. (2010). El viento y la vida de las plantas. *Revista de la Facultad de Ciencias Agrarias UNCuyo, 42*(1), 221-243. https://bdigital.uncu.edu.ar/objetos_digitales/3558/t42-1-r01-golberg.pdf

Gonzales, H. B., Ravi, S., Li, J., & Sankey, J. B. (2018). Ecohydrological implications of aeolian sediment trapping by sparse vegetation in drylands. *Ecohydrology, 11*(7), e1986. https://doi.org/10.1002/eco.1986

Gonzales, H. B., Tatarko, J., & Casada, M. E. (2019). Computational fluid dynamics simulation of airflow through standing vegetation. *Transactions of the ASABE, 62*(6), 1713-1722. https://doi.org/10.13031/trans.13449

Heisler, G. M., & DeWalle, D. R. (1988). Effects of windbreak structure on wind flow. *Agriculture, Ecosystems & Environment, 22-23*, 41-69. https://doi.org/10.1016/0167-8809(88)90007-2

Hong, S. W., Lee, I. B., & Seo, I. H. (2015). Modelling and predicting wind velocity patterns for windbreak fence design. *Journal of Wind Engineering and Industrial Aerodynamics, 142*, 53–64. https://doi.org/10.1016/j.jweia.2015.03.003

Hong, C., Weiwei, H., Chenchen, L., Xueyong, Z., Liqiang, K., Tianle, C., & Kaidi, Z. (2019). Transition model for airflow fields from single plants to multiple plants. *Agricultural and Forest Meteorology*, 266–267, 29-42. https://doi.org/10.1016/j.agrformet.2018.11.039

Instituto Nacional de Vitivinicultura (INV). (2023). *Informe anual de cosecha y elaboración 2023* (Base de datos congelada al 14/09/23). *Anuario de cosecha y elaboración*. https://www.argentina.gob.ar/sites/default/files/2018/10/anuario_cosecha_y_elaboracion_2023.pdf

Judd, M. J., Raupach, M. R., & Finnigan, J. J. (1996). A wind tunnel study of turbulent flow around single and multiple windbreaks, part I: Velocity fields. *Boundary-Layer Meteorology,* 80(1-2), 127–165. https://doi.org/10.1007/bf00119015

Kučera, J., Podhrázská, J., Karásek, P., & Papaj, V. (2020). The effect of windbreak parameters on the wind erosion risk assessment in agricultural landscape. *21*(2020), 150–156. https://doi.org/10.12911/22998993/116323

Lacoste, P. (2019). *La vid y el vino en el Cono Sur de América: Argentina y Chile (1545–2019). Aspectos políticos, económicos, sociales, culturales y enológicos*. Mendoza: Editorial y Talleres Gráficos Cooperativa de Trabajo Ltda.

Lagaglia, F. (2023, September 22). El dato que muestra que en 2023 ya corrió más viento Zonda que en los últimos cuatro años. *MDZ Online*. https://www.mdzol.com/temas/zonda-1835.html

Liu, C., Zheng, Z., Cheng, H., & Zou, X. (2018). Airflow around single and multiple plants. *Agricultural and Forest Meteorology, 252*, 27-38. https://doi.org/10.1016/j.agrformet.2018.01.009

Lyu, J., Wang, C. M., & Mason, M. S. (2020). Review of models for predicting wind characteristics behind windbreaks. *Journal of Wind Engineering and Industrial Aerodynamics, 199*, 104117. https://doi.org/10.1016/j.jweia.2020.104117

Miri, A., Dragovich, D., & Dong, Z. (2017). Vegetation morphologic and aerodynamic characteristics reduce aeolian erosion. *Scientific Reports, 7*(1), 12831. https://doi.org/10.1038/s41598-017-13084-x

Norte, F. A. (1988). *Características del viento zonda en la región de Cuyo* [Doctoral Thesis, Universidad de Buenos Aires] Repositorio de la Universidad de Buenos Aires. https://hdl.handle.net/20.500.12110/tesis_n2131_Norte

Norte, F. A. (2015). Understanding and forecasting Zonda wind (Andean foehn) in Argentina: A review. *Atmospheric and Climate Sciences, 5*, 163-193. http://dx.doi.org/10.4236/acs.2015.53012

Oberschelp, G. P. J., Harrand, L., Mastrandrea, C., Salto, C., & Palenzona, M. (2020). *Cortinas forestales: Rompevientos y amortiguadoras de deriva de agroquímicos*. INTA ediciones.

Otero, F. (2018). *El viento Zonda en Cuyo, características, métodos de clasificación y pronóstico* [Doctoral thesis, Universidad de Buenos Aires] Repositorio de CONICET. https://ri.conicet.gov.ar/handle/11336/84126

Patankar, S. V., & Spalding, D. B. (1972). *Numerical prediction of some three-dimensional fluid flows*. Heat Transfer Section Report Number HTS/72/4, Imperial College.

Peri, P. L. (2003). *Cortinas forestales cortaviento*. EEA Santa Cruz, INTA. https://repositorio.inta.gob.ar/handle/20.500.12123/11531

Phillips, D. A., & Soligo, M. J. (2019). *Will CFD ever replace wind tunnels for building wind simulations? International journal of high-rise buildings, 8*(2), 107-116.

Ramilo, D. I. (2022). Cortinas forestales. In S. E. Sharry, R. A. Stevani, & S. P. Galarco (Eds.), *Sistemas agroforestales en Argentina* (pp. 87-132). Editorial de la Universidad Nacional de La Plata (EDULP). http://sedici.unlp.edu.ar/handle/10915/131898

Rosenfeld, M., Marom, G., & Bitan, A. (2010). Numerical simulation of the airflow across trees in a windbreak. *Boundary-Layer Meteorology, 135*(1), 89-107. https://doi.org/10.1007/s10546-009-9461-8

Stredová, H., Podhrazská, J., Litschmann, T., Středa, T., & Rožnovský, J. (2012). Aerodynamic parameters of windbreak based on its optical porosity. *Contributions to Geophysics and Geodesy, 42*(3), 213–226. https://doi.org/10.2478/v10126-012-0008-5

Tubs (2011, October 18). Mendoza in Argentina [Map]. *Wikimedia Commons*. https://commons.wikimedia.org/wiki/File:Mendoza_in_Argentina.svg

Wang, H., & Takle, E. S. (1997). Model-Simulated Influences of Shelterbelt Shape on Wind-Sheltering Efficiency. *J. Appl. Meteor. Climatol.*, 36, 695–704. https://doi.org/10.1175/1520-0450-36.6.695

Wang, J., Patruno, L., Zhao, G., & Tamura, Y. (2024). Windbreak effectiveness of shelterbelts with different characteristic parameters and arrangements by means of CFD simulation. *Agricultural and Forest Meteorolggogy, 344*, 109813. https://doi.org/10.1016/j.agrformet.2023.109813

Yukhnovskyi, V., Polishchuk, O., Lobchenko, G., Khryk, V., & Levandovska, S. (2020). Aerodynamic properties of windbreaks of various designs formed by thinning in central Ukraine. *Agroforestry Systems*. https://doi.org/10.1007/s10457-020-00503-8